Research on Control of Permanent Magnet Synchronous Motor Based on Second-Order Sliding Mode

Yunkun Sun[1, 2], Qiang Cui[2], and Ye Yuan[2, *]

Abstract—In this paper, a control strategy based on second-order sliding mode is proposed for a permanent magnet synchronous motor (PMSM) drive system applying direct torque control with space vector modulation (DTC-SVM). This control strategy combines the principles of super-twisting algorithms, direct torque control, and space vector modulation, designed to overcome some obvious shortcomings, such as the large ripple of flux linkage and torque in traditional DTC, the poor robustness of traditional PI controllers, and the chattering of traditional sliding mode control. It gives the system good steady state and dynamic performance. The results show that the proposed method effectively solves the above shortcomings. Meanwhile, the control strategy effectively accelerates the dynamic response ability of the system and improves the robustness to parameter perturbation.

1. INTRODUCTION

Direct torque control (DTC) [1–3] is an emerging high-performance AC variable frequency speed control after vector control technology [4] in recent years. Hysteresis comparator is often used to control flux and torque in traditional DTC. However, there is a threshold in hysteresis comparator, and only eight states of voltage inverters can be selected. When the torque or stator flux changes from a very small value to another very small value, the voltage inverter switch does not change, resulting in the voltage vector continuing to function until the error between the given torque and actual torque and the error between the given stator flux and actual stator flux reach the threshold value of hysteresis comparator. This error is especially evident in the low-speed operation or start-up state of the motor [5].

In order to solve these problems in the traditional DTC, scholars have proposed various improvement programs. Refs. [6–8] propose duty cycle modulation for selected voltage vectors, which use respectively simplified duty cycle regulator, PI regulator, and adaptive saturation integral controller to improve the steady-state performance of the system. However, these methods have limited improvement in system performance, and there are many problems such as complex duty cycle solution. Meanwhile, the weight coefficient of the torque ripple and flux linkage on the control system does not adjust the respective weight coefficients in time with the change of the system index, which results in the duty cycle not being the optimal value. Ref. [9] divides the flux linkage error into several levels, which can describe, in more detail, the degree to which the system needs to increase or decrease the torque or flux linkage. At the same time, the duty cycle is discretized, and on this basis, vectors of different amplitudes and phase angles are generated as candidate vectors, which extends the traditional DTC switch table. However, when the motor runs at low speed, the pulsation caused by the hysteresis control of the torque and the stator flux linkage will affect the magnetic flux change of the stator winding, and eventually the torque ripple will be severe. Refs. [10–12] consider the use of multi-level control power converters, which can make multiple spatial voltage vectors act on the motor. This method makes the

flux linkage and torque in the DTC system smooth, and the total harmonic distortion is small, but it greatly increases the hardware cost and complexity of the system. Ref. [13] uses the Space Vector Modulation (SVM) method to make the inverter switching frequency constant to reduce torque ripple. This solution usually uses PI regulator instead of hysteresis regulator to control stator flux and torque, but the selected regulator has the problem of weak robustness. Therefore, [14–16] use Sliding Mode Control (SMC) to solve the problems of traditional DTC torque and flux linkage pulsation, and inverter switching frequency is not constant; however, the sliding mode controller itself has problems of obvious chattering.

In order to solve the above problems, this paper proposes a direct torque control strategy based on second-order sliding mode [17, 18]. The second-order sliding mode is constructed by using super-twisting algorithm [19]. The high-order sliding mode can effectively suppress chattering on the basis of retaining the advantages of the traditional sliding mode. Different from the first derivative of the traditional sliding mode acting on the sliding mode variable, the main idea of the high-order sliding mode is to apply the switching function that generates the buffeting to the high-order derivative of the selected sliding mode variable. The second-order sliding mode algorithm is based on the super-twisting algorithm [20, 21], and its implementation does not require the derivative of the sliding mode variable, thus simplifying the controller structure.

In addition to the second-order sliding mode controller on the torque and flux controller, the traditional PI speed controller is also changed to use the second-order sliding mode controller. In this paper, the speed controller is taken as an example to introduce its construction principle in detail, and its stability and robustness are proved. Moreover, the traditional flux linkage observation scheme usually uses a pure integrator for the convenience of calculation, which has obvious DC offset phenomenon. In order to solve this shortcoming, this paper also gives an improvement on the flux linkage observation scheme. Saturation feedback is added on the basis of the pure integrator, which effectively solves the DC drift phenomenon of the flux linkage. The results show that the system overcomes the shortcomings of traditional PI controller, traditional sliding mode control, and traditional DTC in response speed and torque of the rotating speed and ripple performance of the flux linkage. The method not only effectively improves the ripple of the flux linkage and torque, but also ensures that the switching frequency of the inverter is nearly constant.

2. DESIGN OF CONTROLLER BASED ON SECOND-ORDER SLIDING MODE

2.1. Principle of Sliding Mode Control Based on Super-Twisting Algorithm

The nonlinear dynamic system with single input is as follows.

$$\begin{cases} \dot{x} = f(x) + g(x)u \\ y = s(x,t) \end{cases} \tag{1}$$

where $x \in R^n$ is the state variable. $u \in R$ is the input variable. $f(x)$ and $g(x)$ are uncertain smooth functions. $y = s(x,t)$ is the output variable, i.e., the sliding mode variable.

The super-twisting algorithm is composed of a continuous function and a discontinuous differential with respect to the sliding mode variable, and the continuous function plays a role in the system state arrival phase. Its control law U is as follows.

$$\mathbf{U} = \begin{cases} u_1 = -K_1|s|^{\frac{1}{2}}\text{sgn}(s) + u_2 \\ \dot{u}_2 = -K_2\text{sgn}(s) \end{cases} \tag{2}$$

Compared with the state variable u_1 convergence deviation of traditional first-order sliding mode being proportional to τ (τ is the sample time), the super-twisting algorithm has a convergence deviation of the state variable u_1 in the discrete domain proportional to τ^2, which makes it have more accurate tracking performance.

2.2. Design of Speed Controller Based on Second-order Sliding Mode and Its Stability Analysis

2.2.1. Design Principle of Speed Controller

In the direct torque control system of PMSM, speed outer loop, torque closed loop, and flux closed loop control are adopted.

Taking the design of the outer ring of speed as an example, a second-order sliding mode speed controller is used to make the angular velocity ω_r track the target angular velocity ω_r^* in real time. The speed error is expressed as follows

$$e = \omega_r^* - \omega_r \tag{3}$$

Combined with the PMSM rotor dynamics Equation (4)

$$T_e - T_L - B\omega_r = J\frac{d\omega}{dt} \tag{4}$$

To simplify the controller design, Equation (4) is converted to the following form.

$$\dot{x} = u + d \tag{5}$$

where $u = \frac{T_e}{J}$, $d = -\frac{1}{J}(T_L + B\omega_r)$. T_e is the electromagnetic torque. T_L is the load torque. B is the coefficient of friction of the motor. J is the moment of inertia. ω_r is the mechanical angular velocity. Taking the sliding surface $s = e$, the speed controller designed by the super-twisting algorithm is as follows.

$$\begin{cases} T_e = J\left[-k_1 |s|^{1/2} \operatorname{sgn}(s) + u_2\right] \\ \dot{u}_2 = -k_2 \operatorname{sgn}(s) \end{cases} \tag{6}$$

Let $s = u_1$, $\mathbf{U} = [u_1 \ u_2]^T$, and derive the $\mathbf{U}$, then the closed-loop system equation is as follows.

$$\dot{\mathbf{U}} = \begin{bmatrix} \dot{u}_1 \\ \dot{u}_2 \end{bmatrix} = \begin{bmatrix} -k_1|u_1|^{1/2}\operatorname{sgn}(u_1) + u_2 \\ -k_2\operatorname{sgn}(u_1) \end{bmatrix} \tag{7}$$

Analysing Equation (7) can be concluded that the stability analysis of the closed-loop system is converted to solve the positive definite problem at the equilibrium point.

2.2.2. Stability Analysis of Speed Controller

To prove the stability of the system shown in Equation (7), the Lyapunov function is selected as follows.

$$V = \xi^T P\xi = 2k_2 |u_1| + \frac{1}{2}u_2^2 + \frac{1}{2}\left[k_1 |u_1|^{1/2} \operatorname{sgn}(u_1) - u_2\right]^2 \tag{8}$$

where $\xi^T = [\xi_1 \ \xi_2] = [|u_1|^{1/2}\operatorname{sgn}(u_1) \ u_2]$, $P = \begin{bmatrix} 2k_2 + k_1^2/2 & -k_1/2 \\ -k_1/2 & 1 \end{bmatrix}$, then there is

$$\dot{\xi} = \begin{bmatrix} \frac{1}{2}u_1^{-1/2}\operatorname{sgn}(u_1)^{3/2} \cdot \dot{u}_1 \\ \dot{u}_2 \end{bmatrix}$$

$$= |u_1|^{-1/2} \begin{bmatrix} \frac{1}{2}[-k_1|u_1|^{1/2}\operatorname{sgn}(u_1) + u_2] \\ k_2|u_1|^{1/2}\operatorname{sgn}(u_1) \end{bmatrix}$$

$$= |u_1|^{-1/2} \begin{bmatrix} -\dfrac{k_1}{2} & \dfrac{1}{2} \\ -k_2 & 0 \end{bmatrix} \begin{bmatrix} |u_1|^{1/2}\operatorname{sgn}(u_1) \\ u_2 \end{bmatrix}$$

$$= \frac{1}{|\xi_1|}A\xi \tag{9}$$

where $A=\begin{bmatrix} -k_1/2 & 1/2 \\ -k_2 & 0 \end{bmatrix}$. Deriving Equation (8), while considering Equation (9), can derive Equation (10).

$$
\begin{aligned}
\dot{V} &= \dot{\xi}^{\mathrm{T}}P\xi + \xi^{\mathrm{T}}P\dot{\xi} \\
&= \frac{1}{|\xi_1|}\xi^{\mathrm{T}}A^{\mathrm{T}}P\xi + \xi^{\mathrm{T}}P \cdot \frac{1}{|\xi_1|}A\xi \\
&= \frac{1}{|\xi_1|}\xi^{\mathrm{T}}(A^{\mathrm{T}}P + PA)\xi
\end{aligned}
\tag{10}
$$

Let $Q = -(A^{\mathrm{T}}P + PA) = -\begin{bmatrix} -k_1k_2 - k_1^3/2 & k_1^2/2 \\ k_1^2/2 & -k_1/2 \end{bmatrix}$. It can be found that when k_1 and $k_2 > 0$, there must be a negative symmetric matrix of Q. At this time, the constructed Lyapunov function $V > 0$, $\dot{V} < 0$, that is, the system in Eq. (7) is globally stable. Therefore, under the action of the second-order sliding mode speed controller in Eq. (6) based on the super-twist algorithm, the system in Eq. (5) can be made in a global stable state.

Similarly, in the rotating coordinate system dq, according to the flux amplitude equation and electromagnetic torque equation of surface mounted PMSM (11),

$$
\begin{cases}
\dfrac{\mathrm{d}}{\mathrm{d}t}|\psi_{\mathrm{s}}| = u_d - R_{\mathrm{s}}i_d \\[2mm]
\dfrac{\mathrm{d}}{\mathrm{d}t}T_{\mathrm{e}} = \dfrac{3}{2}p_{\mathrm{n}}\psi_{\mathrm{f}} \cdot \dfrac{1}{L_s}\left(u_q - R_{\mathrm{s}}i_q - \omega_{\mathrm{e}}\psi_{\mathrm{f}}\right)
\end{cases}
\tag{11}
$$

where u_d and u_q are the stator voltage components in the d-q coordinate system. i_d and i_q are the stator current components in the d-q coordinate system. $|\psi_s|$ is the stator flux linkage vector magnitude. L_s is the stator inductance. ψ_{f} is the permanent magnet flux linkage amplitude. R_{s} is the stator resistance. ω_{e} is the electrical angular velocity. p_n is the polar number of the motor.

The corresponding torque and flux controller can be designed as follows.

$$
\begin{cases}
\psi_{\mathrm{s}} = k_3|s_{\psi_{\mathrm{s}}}|^{1/2}\mathrm{sgn}(s_{\psi_{\mathrm{s}}}) + \displaystyle\int_0^t k_4\mathrm{sgn}(s_{\psi_{\mathrm{s}}})\mathrm{d}t \\[2mm]
T_{\mathrm{e}} = k_5|s_{T_{\mathrm{e}}}|^{1/2}\mathrm{sgn}(s_{T_{\mathrm{e}}}) + \displaystyle\int_0^t k_6\mathrm{sgn}(s_{T_{\mathrm{e}}})\mathrm{d}t
\end{cases}
\tag{12}
$$

where $s_{\psi_{\mathrm{s}}}=\psi_{\mathrm{s}}^* - \psi_{\mathrm{s}}$, $s_{T_{\mathrm{e}}}=T_{\mathrm{e}}^* - T_{\mathrm{e}}$, that is, the sliding mode surfaces of the flux linkage and the torque respectively.

2.3. Robustness Analysis of Speed Controller

When the system is actually running, it will be affected by internal parameter perturbation, external interference, measurement error, and measurement noise. The equation of the speed considering the interference can be expressed as follows.

$$
\frac{\mathrm{d}}{\mathrm{d}t}\omega_r = \frac{1}{J}(T_{\mathrm{e}} - T_{\mathrm{L}} - B\omega_r) + \sigma
\tag{13}
$$

where σ is the interference term. Combination Eqs. (6) and (12),

$$
\frac{\mathrm{d}s}{\mathrm{d}t} = k_1|s|^{1/2}\mathrm{sgn}(s) - \int_0^t k_2\mathrm{sgn}(s)\mathrm{d}t + \frac{1}{J}(T_{\mathrm{L}} + B\omega_r) + \sigma
\tag{14}
$$

Select $|\sigma| \le \kappa|u_1|^{1/2}$, $\kappa = \max|-\frac{1}{J}(T_{\mathrm{L}} + B\omega_r)|$ with $k_1, k_2 > 0$ the speed control system considering that the interference remains stable, that is, the permanent magnet synchronous motor speed control system designed in this paper is still robust. For the same reason, reference can be made to the above analysis method to prove that the corresponding torque control system and flux linkage control system are also robust, not tired in words here.

2.4. Improvement of Stator Flux Linkage Estimation

In the traditional DTC method, the stator flux linkage voltage integration method is adopted. Although the calculation is simple, the pure integrator has problems such as integral initial value and DC offset. In order to solve the shortcomings of this pure integrator, saturation feedback can be added to it.

The output form of the improved integrator is as follows

$$y = \frac{1}{s + \omega_c} x + \frac{\omega_c}{s + \omega_c} z \qquad (15)$$

where z is the output of the saturated module, and $|z|_{\max} = L$.

Assuming that the input is a pure DC signal, the maximum output of the integrator is as follows.

$$y_{dc} = \frac{1}{\omega_c} x_{dc} + L \qquad (16)$$

Equation (16) shows that the improved integrator does not cause saturation, proving that the setting of L is reasonable.

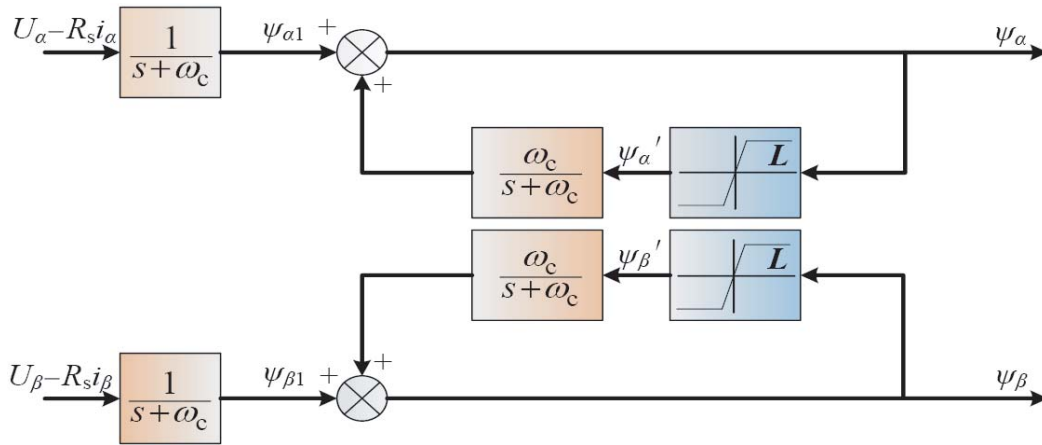A block diagram of stator flux estimation with saturated feedback is shown in Fig. 1.

Figure 1. Block diagram of stator flux linkage estimation based on saturated feedback.

To eliminate the DC component in the output, set L equal to the magnitude of the actual flux linkage. If L is greater than the amplitude of the actual flux linkage, it will cause the output flux linkage waveform to produce a DC offset. If L is less than the actual flux amplitude, the output flux waveform does not contain any DC offset, but it is distorted.

3. PERMANENT MAGNET SYNCHRONOUS MOTOR CONTROL SYSTEM BASED ON SOSM

The control block diagram of the permanent magnet synchronous motor based on second-order sliding mode proposed in this paper is shown in Fig. 2(a), and Fig. 2(b) shows the block diagram of the second-order sliding mode controller based on super-twisting algorithm. The controller combines the principles of super-twisting algorithm, direct torque control, and space vector modulation to achieve simple and effective control of speed, torque, and flux linkage.

4. RESULTS AND ANALYSIS

In order to verify the validity of the designed controller, a simulation model is established by using MATLAB/Simulink. The motor parameters in the simulation are shown in Table 1. The sampling
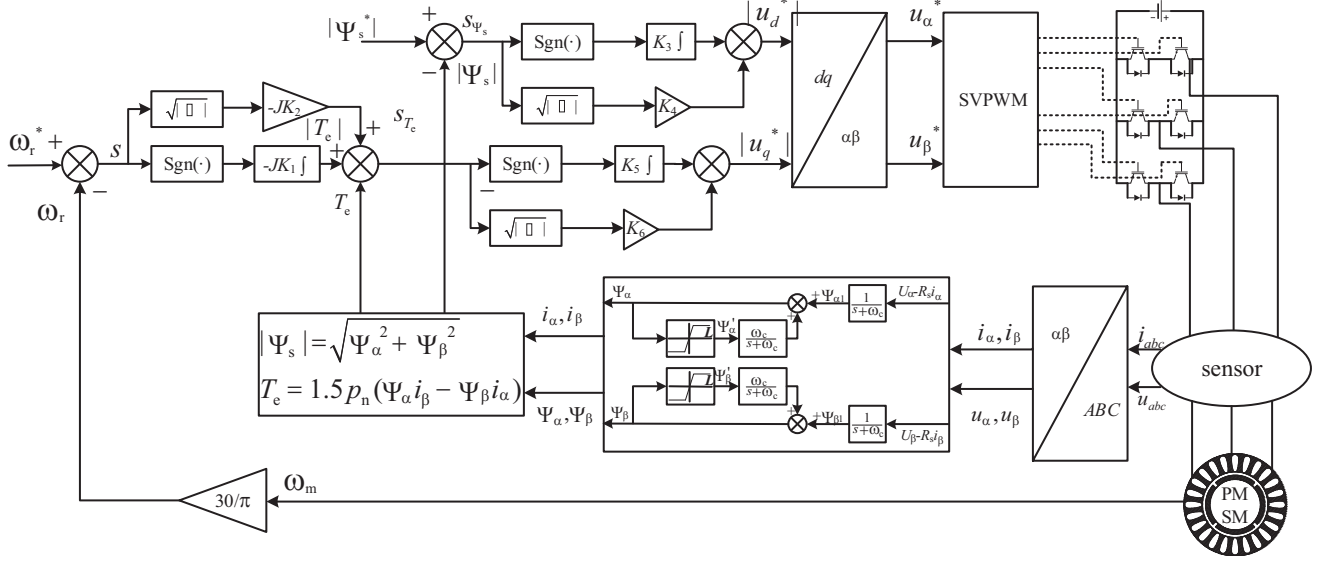
Figure 2. Control block diagram of permanent magnet synchronous motor based on second-order sliding mode.

Table 1. Simulation parameters of PMSM.

Parameter	Value	Parameter	Value
Rating voltage U_N	311 V	Stator phase resistance R_s	$1.2\,\Omega$
Rating speed n_N	600 r/min	Moment of inertia J	$0.008\,\text{kg} \cdot \text{m}^2$
Rating torque T_N	$3\,\text{N} \cdot \text{m}$	Number of pole pairs p_n	4
Stator inductance L_s	0.0085 H	Permanent magnet flux linkage ψ_f	0.175 Wb

mode is fixed step ode3. Given the flux linkage magnitude $|\psi_{s|=0.3\text{Wb}}$, the simulation data can be obtained.

Firstly, under the traditional DTC algorithm, the flux linkage observer integrating the ordinary voltage model is compared with the improved flux observer of the paper (taking ψ_a as an example). The cutoff frequency of flux saturation feedback ω_c is 40 Hz. Fig. 3 shows the waveforms of the flux linkage observations of the two.
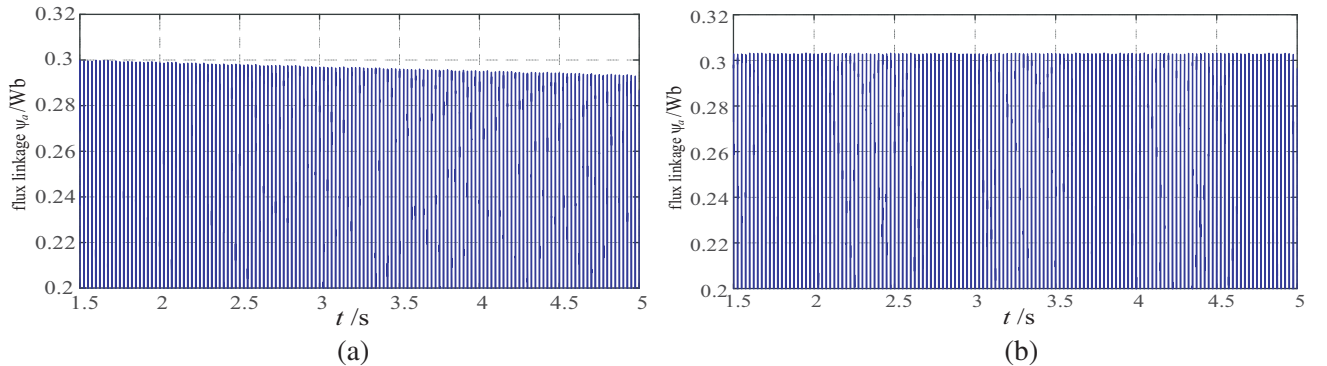

Figure 3. Comparison of flux ψ_a estimation results under two integrators. (a) Output flux of the pure integrator. (b) Output flux of the integrator with saturated feedback.

It can be seen from Fig. 3 that the improved flux linkage observation method can obviously solve the DC offset defect of the pure integrator. Therefore, the improved flux linkage observation method has better flux linkage tracking performance.

The direct torque control based on the Super Twisting-Second Order Sliding Mode (ST-SOSM) designed in this paper is compared with the traditional DTC algorithm. Fig. 4 shows the steady-state waveforms of the two methods at a motor speed of 600 r/min without load disturbance.
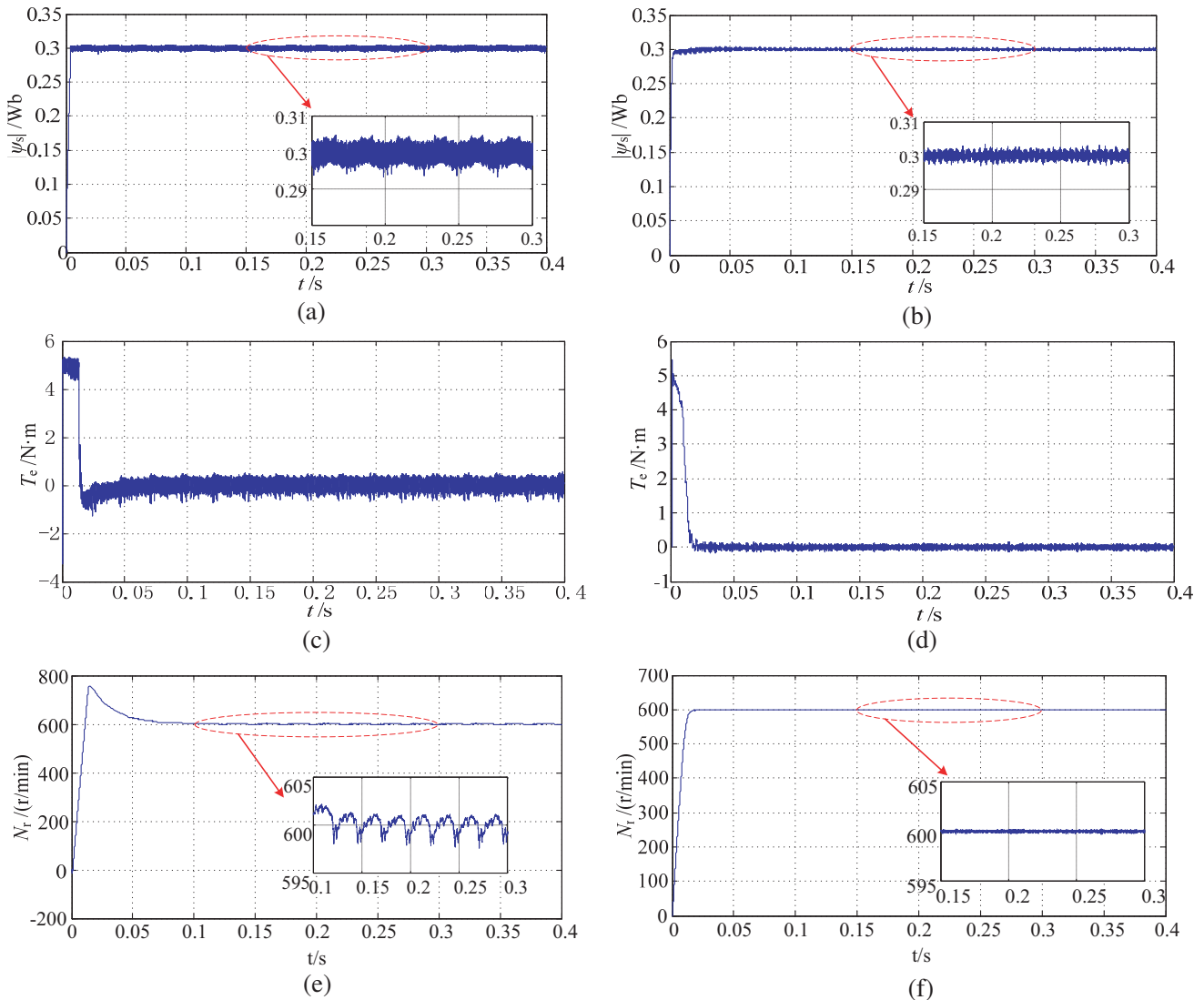

Figure 4. Comparison of flux, torque, and speed steady state waveforms under traditional DTC and ST-SOSM. (a) Steady state flux linkage waveform under traditional DTC. (b) Steady state flux linkage waveform under ST-SOSM. (c) Steady-state torque waveform under traditional DTC. (d) Steady-state torque waveform under ST-SOSM. (e) Steady-state speed waveform under traditional DTC. (f) Steady-state speed waveform under ST-SOSM.

It can be seen from Fig. 4 that the torque and flux linkage waveforms are smooth during the steady-state operation; the speed waveform response is rapid, no ripple; and the overshoot is small, which has obvious advantages over the traditional DTC. Therefore, the second-order sliding mode-based control algorithm has a faster response speed and better flux linkage and torque ripple suppression under steady-state operation of the motor without load disturbance.
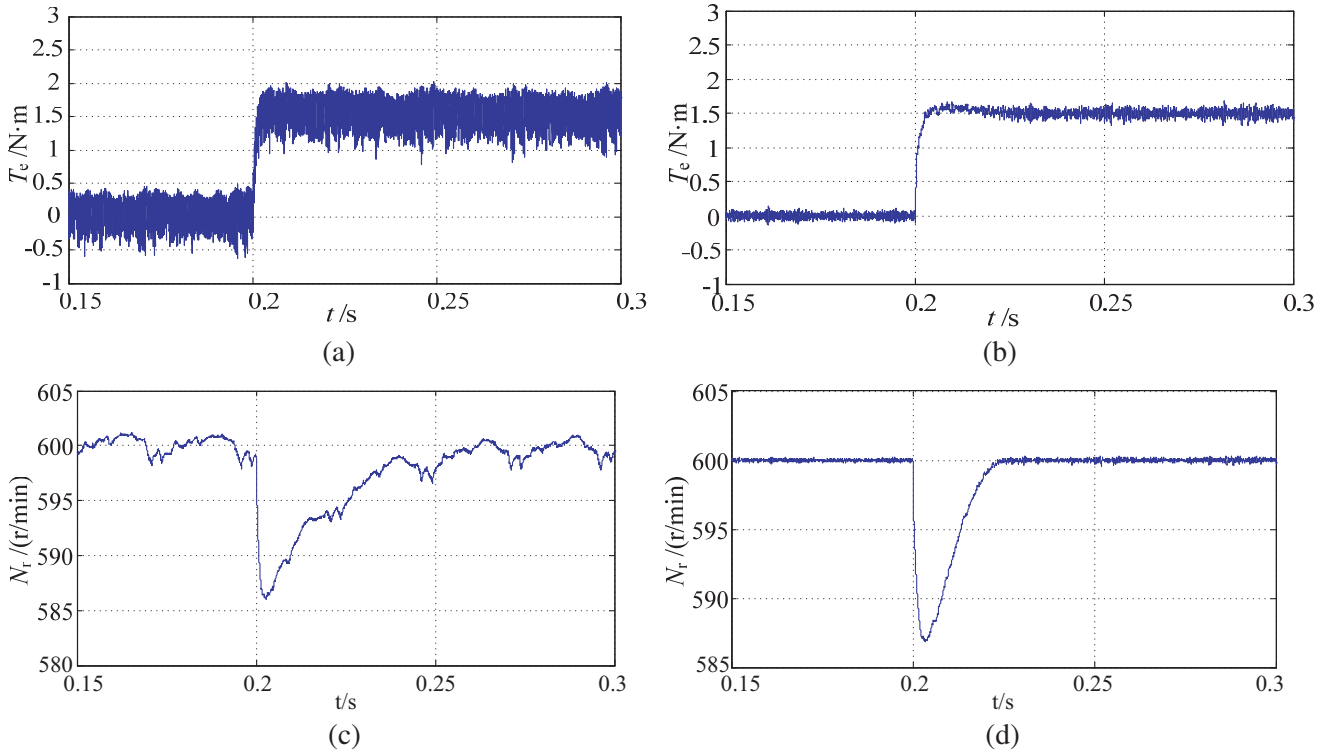
Figure 5. Dynamic waveforms of flux, torque and speed under traditional DTC and ST-SOSM. (a) Dynamic torque waveform under traditional DTC. (b) Dynamic torque waveform under ST-SOSM. (c) Dynamic speed waveform under traditional DTC. (d) Dynamic speed waveform under ST-SOSM.

Figure 5 shows the dynamic waveforms of $1.5\,\text{N}\cdot\text{m}$ load added suddenly at $t = 0.2\,\text{s}$ when the motor speed is $600\,\text{r/min}$.

It can be seen from Fig. 5 that the robustness of the designed ST-SOSM-based direct torque control system is improved compared with the traditional DTC algorithm and the traditional PI controller, regardless of the speed or torque waveform.

5. CONCLUSION

In order to overcome the shortcomings of poor control of DTC-SVM and chattering shortcomings of traditional SMC, this paper proposes a permanent magnet synchronous motor control system based on second-order sliding mode. The speed outer ring, magnetic link ring, and torque ring are replaced by a second-order sliding mode controller instead of the conventional PI controller. Among them, the combination of sliding mode control and inverter switching characteristics effectively improves the dynamic performance of the system, while space vector modulation ensures the steady state performance of the system. The results show that the proposed method effectively reduces the flux linkage and torque ripple, improves the response speed of the rotating speed, and has strong robust performance to the changes of system parameters.

ACKNOWLEDGMENT

REFERENCES

1. Shankar, V. K. A., S. Umashankar, and S. Paramasivam, "Investigations on performance evaluation of VFD fed PMSM using DTC control strategies for pumping applications," *Conference on Innovations in Power and Advanced Computing Technologies*, Apr. 2017.

2. Niu, F., B. S. Wang, A. S. Babel, K. Li, and E. G. Strangas, "Comparative evaluation of direct torque control strategies for permanent magnet synchronous machines," *IEEE Transactions on Power Electronics*, Vol. 31, No.2, 1408–1424, Feb. 2016.

3. Zhu, H. Q. and Y. Xu, "Development of bearingless permanent magnet synchronous motor system and key technologies," *Proceedings of the CSEE*, Nov. 28, 2018.

4. Bida, V. M., D. V. Samokhvalov, and F. S. Al-Mahturi, "PMSM vector control techniques — A survey," *IEEE Conference of Russian Young Researchers in Electrical and Electronic Engineering*, Jan. 2018.

5. Yuan, T. Q. and D. Z. Wang, "Performance improvement for PMSM DTC system through composite active vectors modulation," *Electronics*, Vol. 7, No. 10, Oct. 2018.

6. Zhang, Y., J. Zhu, W. Xu, et al., "A simple method to reduce torque ripple in direct torque-controlled permanent-magnet synchronous motor by using vectors with variable amplitude and angle," *IEEE Transactions on Industrial Electronics*, Vol. 58, No. 7, 2848–2859, 2011.

7. Niu, F. and K. Li, "Direct torque control for permanent magnet synchronous machines based on duty ratio modulation," *IEEE Transactions on Industrial Electronics*, Vol. 62, No. 10, 6160–6170, 2015.

8. Zhang, Z., C. Wei, W. Qiao, et al., "Adaptive saturation controller-based direct torque control for permanent magnet synchronous machines," *IEEE Transactions on Power Electronics*, Vol. 31, No. 10, 7112–7122, 2016.

9. Xiao, M., T. Shi, Z. Wang, et al., "Direct torque control for permanent magnet synchronous motor with multilevel hysteresis controller," *Proceedings of the CSEE*, Vol. 37, No. 14, 4201–4211, 2017.

10. Atallah, A. M. and E. I. Tantawy, "Direct torque control of machine side multilevel converter for variable speed wind turbines," *Energy*, Vol. 90, 1091–1099, Oct. 2015.

11. Islam, M. D., C. M. F. S. Reza, and S. Mekhilef, "Modeling and experimental validation of 5-level hybrid H-bridge multilevel inverter fed DTC-IM drive," *Journal of Electrical Engineering & Technology*, Vol. 10, No. 2, 574–585, Mar. 2015.

12. Lakshmi, G. S. and K. Navya, "Multilevel diode-clamped inverter fed IPMSM drive for electric traction," *International Conference on Innovations in Electrical, Electronics, Instrumentation and Media Technology*, Feb. 2017.

13. Qiu, X., W. Huang, J. Yang, and F. Bu, "A direct torque control strategy based on torque angle for permanent magnet synchronous motors," *Transactions of China Electrotechnical Society*, Vol. 28, No. 10, 56–62, Mar. 2013.

14. Cristian, L., B. Ion, and B. Frede, "Comparative analysis of direct torque control and DTC based on sliding mode control for PMSM drive," *29th Chinese Control and Decision Conference*, May 2017.

15. Fan, Y., X. F. Zhou, X. Y. Zhang, L. Zhang, and M. Cheng, "Sliding mode control of IPMSM system based on a new reaching law and a hybrid speed controller," *Transactions of China Electrotechnical Society*, Vol. 32, No. 5, 9–18, 2017.

16. Zhang, X. G., K. Zhao, L. Sun, et al., "Sliding mode control of permanent magnet synchronous motor based on a novel exponential reaching law," *Proceedings of the CSEE*, Vol. 31, No. 15, May 2011.

17. Shi, S., S. Y. Xu, B. Y. Zhang, Q. Ma, and Z. Q. Zhang, "Global second-order sliding mode control for nonlinear uncertain systems," *International Journal of Robust and Nonlinear Control*, Vol. 29, No. 1, 224–237, Jan. 2019.

18. Orlov, Y., A. Pisano, S. Scodina, and E. Usai, "On the Lyapunov-based second-order SMC design for some classes of distributed parameter systems," *IMA Journal of Mathematical Control and Information*, Vol. 29, No. 4, 437–457, Dec. 2012.

19. Castillo, I., L. Fridman, and J. A. Moreno, "Super-Twisting Algorithm in presence of time and state dependent perturbations," *International Journal of Control*, Vol. 91, No. 11, 2535–2548, Nov. 2018.

20. Gonzalez, J. A., A. Barreiro, S. Dormido, and A. Banos, "Nonlinear adaptive sliding mode control with fast non-overshooting responses and chattering avoidance," *Journal of the Franklin Institute — Engineering and Applied Mathematics*, Vol. 354, No. 7, 2788–2815, May 2017.

21. Zeng, X. F., J. Y. Wang, X. H. Wang, and T. J. Wang, "Design of sliding mode controller based on SMDO and its application to missile control," *Acta Aeronautica ET Astronautica Sinica*, Vol. 32, No. 5, May 2011.